# Chapter 16
# Personal/Body Area Networks and Healthcare Applications

## 16.1 Introduction

A personal area network (PAN) is the interconnection of devices for information technology within the range of a single person, characteristically within a range of 10 m, and is typically coupled with wireless links and hence called wireless PAN (WPAN). These devices could be Bluetooth-based or ZigBee, or even new near-field communication components as pico-networks. The emphasis is to use groundbreaking data delivery schemes that could connect various transducers to form a comprehensive team and provide useful information for health care. Ever-increasing cost of health care has become a national concern as Medicare had 35 million members in 2003 and 35.4 million in 2004 (Fig. 16.1). Healthcare expenditures in the USA are projected to rise to 15.9% of the gross domestic product ($2.6 trillion) by 2010. The total cost for cancer treatment in 2020 is projected to be $173 billion, which represents a 39% increase from 2010. In 2013, 14.4 million Medicare beneficiaries are enrolled in Medicare Advantage Plans, an increase of more than 1 million (9.7%) from 2012. A vast majority of beneficiaries (98%) have access to Medicare Advantage Prescription Drug (MA-PD) Plans with no premium. Slightly more than half (55%) of beneficiaries are enrolled in a zero-premium plan in 2013. It is worth noticing that eligibility for Medicare = 65 = senior citizen/geriatric and "old" can be said between 65 and 85 years, while 85 + people can be classified as "very old." There are 700 million seniors worldwide (1.3 billion in 2040), and life expectancy in USA is around 78. So, people at 65 expected to live another 18.7 years. Women outnumber the man in the elderly population and consider a 70-year-old widow living at home all by herself. A lady may have mild cognitive impairment, but does most of the household work on her own and wants to remain as much independent as possible and even wants to help her friends with similar problems (Table 16.1). Multiple chronic illnesses require multiple medications, and if the lady is not taking medications, her condition may become acute. So, there could be one or more side


D.P. Agrawal, *Embedded Sensor Systems*,
DOI 10.1007/978-981-10-3038-3_16

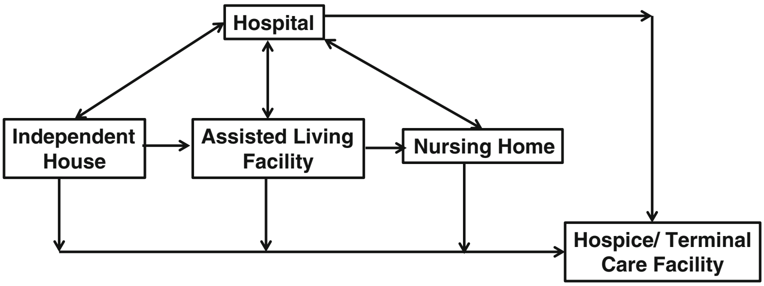


**Fig. 16.1** Elderly people statistics

**Table 16.1** Elderly people and daily activities

| Age | Sensorimotor and cognitive abilities (average) | Deficit (average) | Technology support needed for daily activities |
|---|---|---|---|
| 60–70 | 100–90 | 0–10 | Minimal |
| 70–80 | 70 | 30 | Moderate |
| 80–90 | 50 | 50 | High |
| 90+ | 0–10 | 90–100 | Very high |

effects. There could be a visit from a trained nurse once a week. So, the goal is to manage chronic conditions and delay a move to assisted living/nursing home for 10 years to save around $500,000 in nursing home expenses.

Table 16.2 [reproduced from 1] recapitulates features of different applications based on sampling rate desired, memory size required, communication bandwidth needed, migration of application components, network coverage, and preferred reliability. First of the five types is based on sampling periods varying from one second to few hours to cover a large area with no strict deadlines for the results. These include environmental and agricultural applications. Energy in SNs is expected to last from few days to months and possibly recharged with solar cells. Type 2 applications are defined for smaller space and intensive computing requirements with sampling period varying from 1 ms to 1 s, with possibility of processing being done after storing samples. Type 3 applications, processing of images are desired in Type 2 applications and SNs are synchronized and some mobile units. In type 4 applications, the space is restricted as compared to type 3 and SN energy is expected to last for a week and healthcare application belong to this type. Type 5 is primarily for industrial process control with restricted jitter, and sampling periods vary from 50 ms to few seconds.

**Table 16.2** Application characterization and monitoring rates [1]

| Application | Sampling rate | Possible applications | Computing capacity | Memory size | Communication bandwidth | Location | Mobility of components | Real-time | Network's coverage | Energy autonomy | Synchronization |
|---|---|---|---|---|---|---|---|---|---|---|---|
| Type 1 | 1 s to few hours | Agricultural and environmental applications | Low performance | Low | <256 kbps | Yes | No | Only measurement | Open space 10 km | Months | Yes |
| Type 2 | 1 ms to 1 s | Industrial and agricultural sectors | Low performance | Medium | <256 kbps | Yes | No | Only measurement | Confine space 100 m | There isn't restriction | Yes |
| Type 3 | 1 ms to 1 s | Agricultural sector for detection of pests, and environmental sector aimed at detecting fires | High performance | High | 1 Mbps | Yes | Yes | Only measurement | Open space 10 km | Hours | Yes |
| Type 4 | | Diseases with body area networks | High performance | Medium | <256 kbps | Yes | Yes | Only measurement | Open space 1 km | Days | Yes |
| Type 5 | 50 ms to few seconds | Industrial control process | Low performance | Low | <256 kbps | No | No | End to end and minimum jitter variability | Confine space 100 m | There isn't restriction | Yes |

## 16.2 Activities of Daily Living

Various activities of daily living (ADL) include food, hygiene, social needs, sleep, medications, managing chronic conditions, safety, and financial needs. Elderly people have increased susceptibility to falls, and if living alone, it could be hours or days before someone finds out. This could lead to more health complications, and any delay in treating such illness increases the severity. So, detection of falls is an important requirement, and few options for automatic detection of falls include estimation of posture and pressure on sensor-equipped floors. Visual fall detection is feasible along with context information and is suitable for sensor–motor and cognitive difficulties. One approach could be the use of wearable, portable, and implanted device to recognize the fall. Another simple scheme could be based on computers, Internet, Web sites, cell phones, and alarm system. An intermediate solution could be RFID-based emergency alarm system for medication and task reminder systems. An elaborate system could have a smart home with all clever devices that are reliable, smart and context-aware, personalized, robust, self-configuring, and causing no harm to the patients. The cognitive role could include executive function, decision making, and dual-task performance and could decline with age. An electronic patient record can be kept besides remote patient monitoring. So, for integration of wireless communication, networking and information technology is required and a large volume of medical information can be collected to define most effective strategies for treating chronic illness and reducing disability. Efforts should be made to improve health and reduce healthcare cost, and chronic disease must be managed by the effective use of clinical resources that necessitates a complete integration of IT.

Therefore, wireless communication, sensor platform, networking, and database need to be incorporated in a clinical practice with unequivocal security and privacy rules to protect end-to-end communication and limit access to sensitive medical information. A cellular 3G/4G technology can be used for such application as it provides real-time delivery with wide coverage adequate bandwidth and ability to work with other wireless technologies as they are widely used and are secure with possible location management. The only problems are the presence of dead spots, providing reliability is a real challenge, there is lack of broadcast/multicast, and pricing structure could impact of the commercial traffic. This forces us to consider WLAN for monitoring applications as it provides adequate bit rate, supports transmission from patients to access point (AP), and could prove to be handy for mobile patients as location management is feasible. The limitations are the coverage area, delays in monitoring, associated security, presence of colocated networks, no provision for multicasting, and reliability is questionable. Wireless LANs experience unpredictable coverage , and the data speed is variable as bandwidth needs to be shared and interference may be present with unlicensed ISM band. It may be possible that the device could not access the network as reaching to cellular phone sometimes is difficult and video quality may not be good due to variable delays. A generic telemedicine (Fig. 16.2a) ought to support utilization of different assets

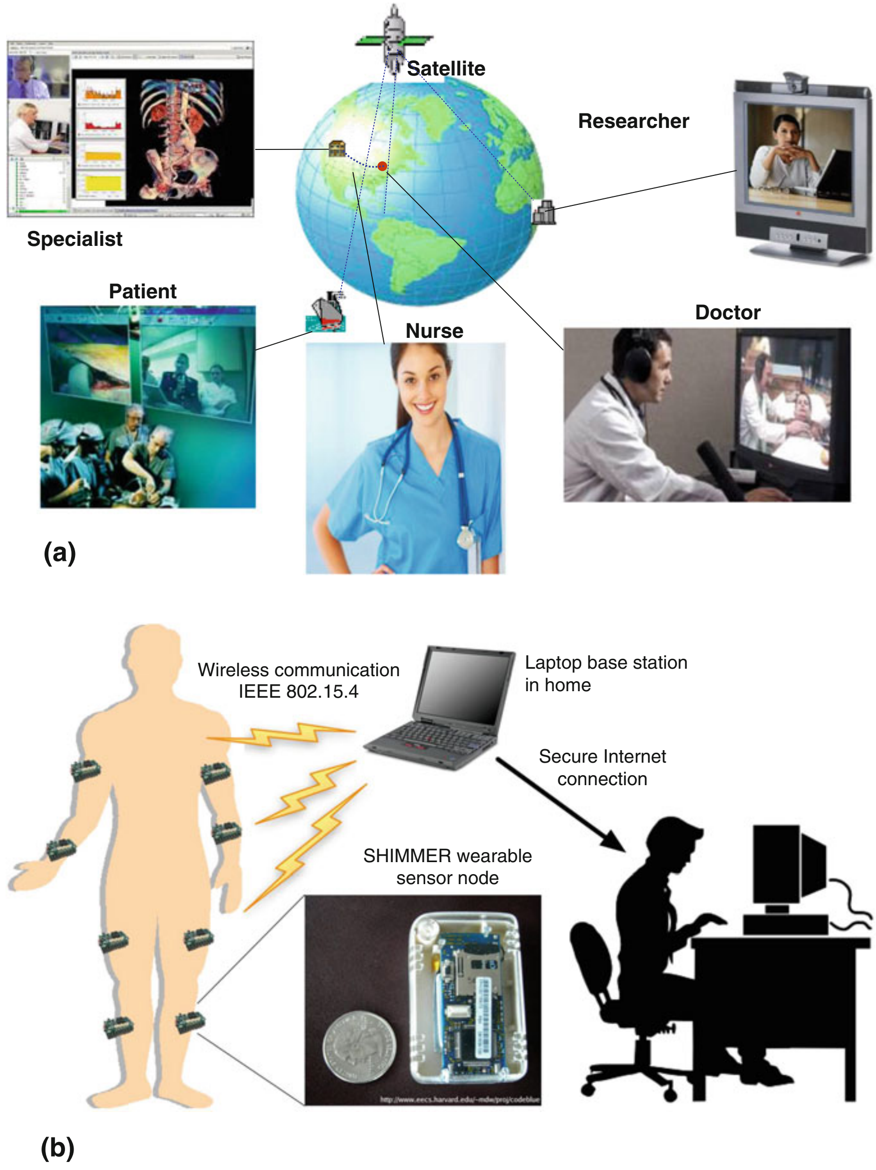


**Fig. 16.2** **a** A generic telemedicine **b** Monitoring Mobility

independent of their geographical location, and there is a need for multidisciplinary collaboration. It is desirable to facilitate dissemination of medical knowledge to practicing doctors and medical students and enable doctors in remote and rural areas to refer with specialists in urban areas.

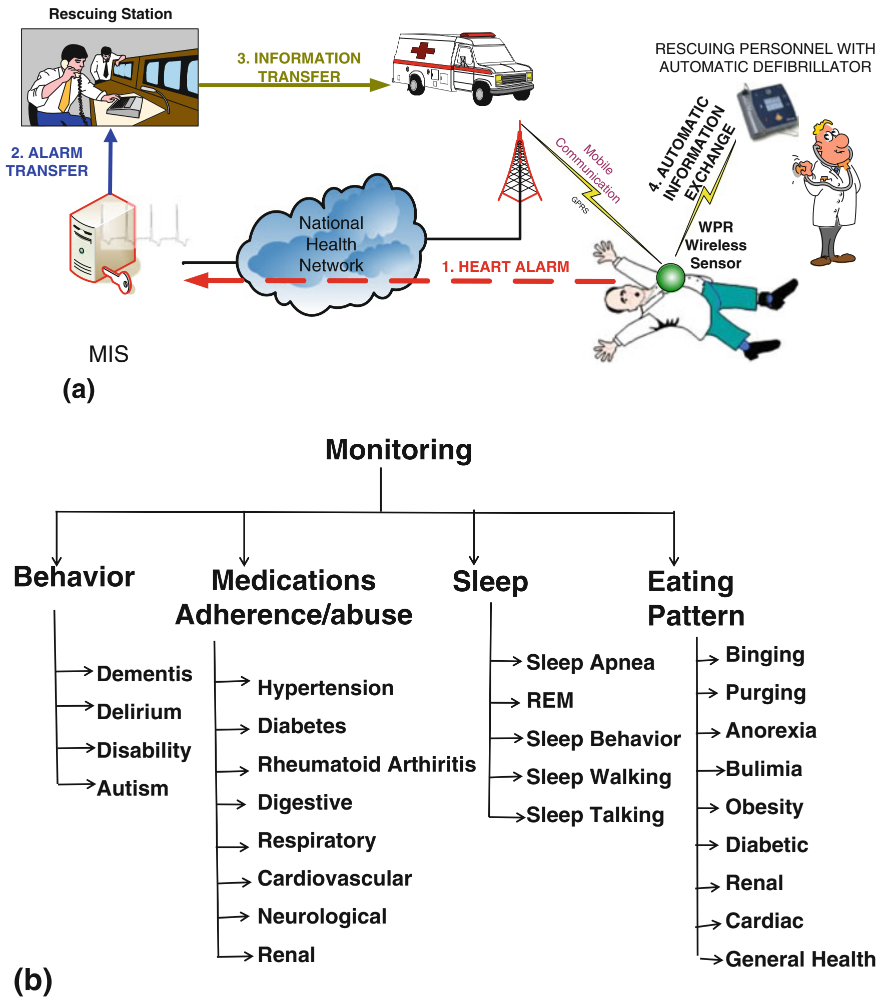


**Fig. 16.3** **a** Emergency Scenario **b** Physiological parameters to be monitored

If the objective is to monitor mobility only, then sensor boards could be attached to legs and hands as shown in Fig. 16.2b. A more chaotic scene appears when an accident occurs (Fig. 16.3a), and every attempt is made to save human life. So, there is a need to monitor many different body parameters as shown in Fig. 16.3b. A personal health monitoring system can be envisioned as illustrated in Fig. 16.4a. Details of used different types of physiological parameters are shown in Fig. 16.4b, while a comprehensive health monitoring system is depicted in Fig. 16.5a, showing utilization of assets independent of their geographical location to constitute a multidisciplinary collaboration.

Functions to be performed and dissemination of knowledge at different facilities to practicing doctors and medical students are shown in Fig. 16.5b. Such an

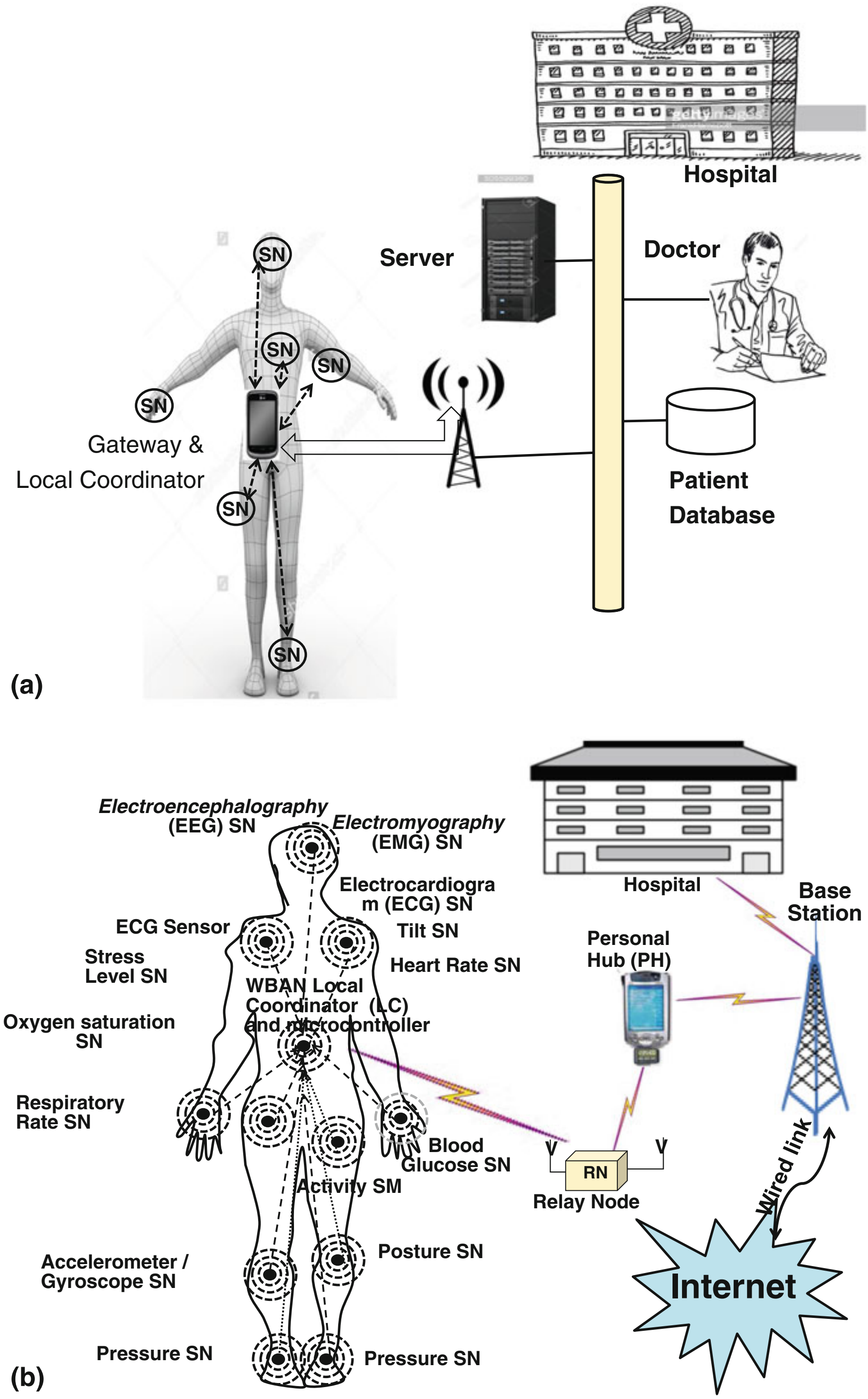


**Fig. 16.4** **a** Personal health monitoring system **b** Detailed health monitoring system

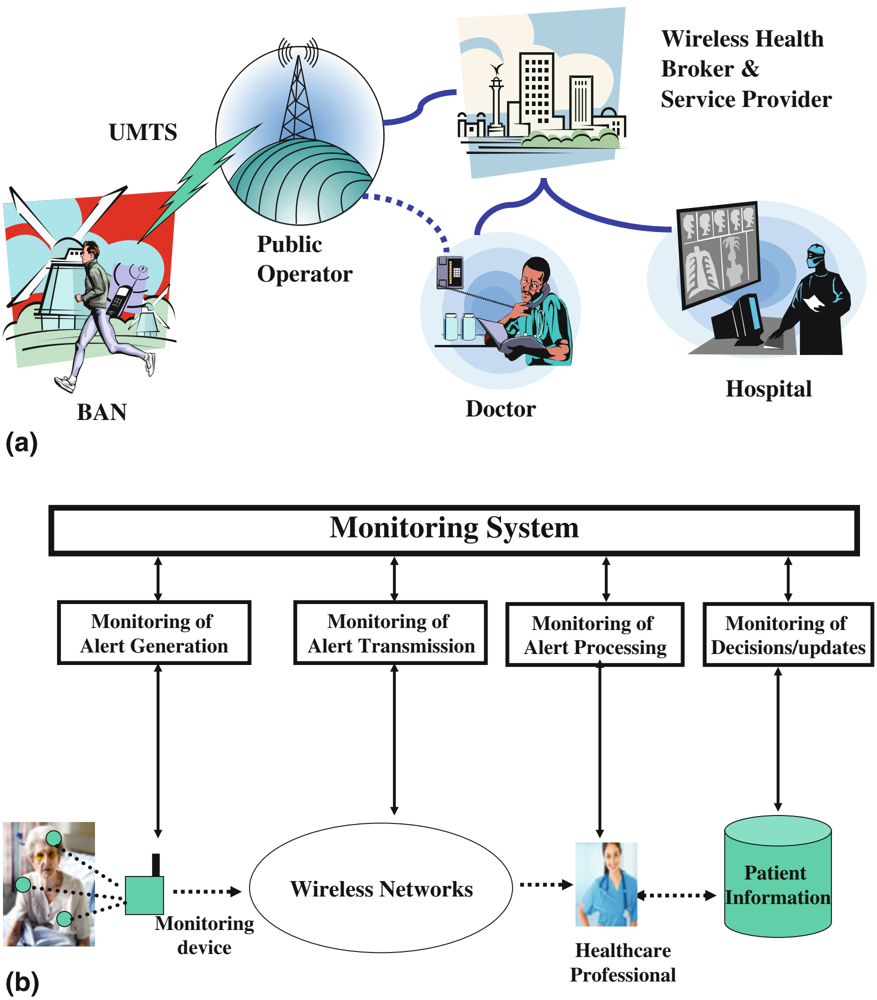


**Fig. 16.5** **a** Scheme for personal health monitoring system **b** Functional details for personal health monitoring system

infrastructure allows doctors in remote and rural areas to consult with specialists in urban areas and take appropriate medical and clinical decisions. So, there is a clear need for intercommunication among medical devices and clinical information systems. This has been accomplished with a number of medical products such as infusion pumps and ventilators that commonly have RS-232 ports, and these devices can communicate with many physiological monitoring instruments. There are several medical equipments that could be easily linked for personal communication. However, virtually, all of these are specialized applications, and unique custom interfaces are needed. To address the medical device plug-and-play interoperability problem, a single communication standard is needed to provide

**Table 16.3** Vital physiological parameters and associated characteristics [2]

| Vital sign and parameters | Sampling rate | Quantization (bits/sample) | Total bit rate |
|---|---|---|---|
| Breathing rate | One sample/sec | 4 | 4 bps |
| ECG | 240 samples/sec | 12–36 | 2.9–8.7 Kbps |
| Blood pressure | One sample/minute | 64 | 1 bps |
| Oxygen saturation | One sample/sec | 16 | 16 bps |
| Core body temperature | One sample/minute | 16 | 0.3 bps |

unobtrusive and persistent monitoring. So, different physiological parameters ought to be monitored, and associated characteristics are summarized in Table 16.3 [2]. Different factors need to be sensed and sent by SNs at dissimilar frequencies, depending on criticality of data.

## 16.3 Available Biomedical Transducers

In biomedical application, the most important issues to tackle are the quality of service (hand-over, interruption/delays in transmission, data loss bandwidth problems, etc.), social acceptance (health risks (cell phone usage), economic issues, ethical issues), and legal issues (accreditation of the devices and applications, protection of health-related data, privacy, security, and encryption of data, and medical responsibilities/liability). There are many commercial products, and they are helping human race. These include (Fig. 16.6) Nokia N810 Internet Tablet, Motion sensor (802.16.4), weight scale (Bluetooth) blood pressure monitor (Bluetooth) device.

Noninvasive technology is also being used to measure the heart rate (HR) and blood oxygen saturation ($SpO_2$) (Fig. 16.7a, b) as it projects infrared and near-infrared light through blood vessels near the skin and by determining the amount of light absorbed by hemoglobin in the blood at two different wavelengths, and the oxygen level can be determined. The heart rate can also be found as the blood vessels contract and enlarge with the patient's pulse. The *Pluto activity center* is useful for patients undergoing physical rehabilitation using long-lasting rechargeable battery.

Many other biomedical devices which use SN as an integral part are shown in Fig. 16.8. Areas that affect human health the most are the ECG (monitoring heart activity), EMG (electromyography), and for sensing motion (activity) and are discussed in some detail here (Fig. 16.9). Electrocardiogram (ECG) SNs require a large bandwidth as parallel transmission of many waveforms is needed. There could be environmental interferences, and patient's movement must be restricted during the test. The drug delivery mechanism is used to respond to any anomalies in the

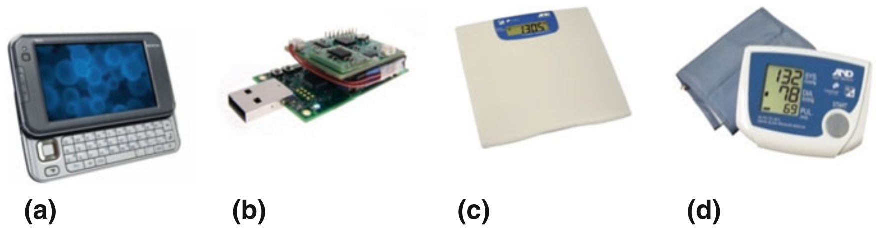


Fig. 16.6 **a** Nokia N810 tablet **b** Motion sensor **c** Weight scale **d** Blood pressure monitor

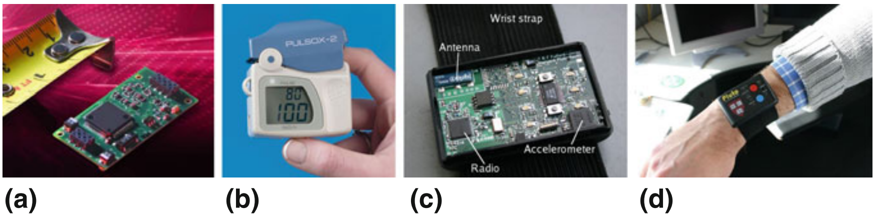


**Fig. 16.7** **a b** Heart rate (HR) and blood oxygen saturation ($SpO_2$) **c d**: *Pluto* Activity Sensors

heart. The detection is based on SQRS Algorithm [3] on ECG waveforms, and misclassification due to noise can be avoided by having an appropriate threshold. The most common type of ECG involves the connection of several leads to a patient's chest, arms, and leg via adhesive foam pads (Fig. 16.10a). The device records a short sample, e.g., 30 s, of the heart's electric activity between different pairs of electrodes. When there is a need to detect irregular cardiac condition, an uninterrupted EKG measurement is adopted. This involves checking for extended period patient's cardiac activity utilizing 2 or 3 electrodes. The ECG signal is small ($\sim$1 mV peak-to-peak) and is amplified (gain >1000) using low-noise amplifiers and filtered to remove noise before being digitized. In Fig. 16.10b, P wave determines contractions of the atria and QRS is a series of waves linked with ventricular contractions. The T and U waves follow the ventricular contractions, and various sampling rates and quantization levels are used with sampling frequencies selected between 128 and 256 Hz. For rigorous details, higher sampling rates and bit rates, e.g., 16 bits, are adopted. IMEC (Fig. 16.10c) [4] has recently developed a wireless, flexible, stretchable EKG patch for continuous cardiac monitoring which can be placed on the arm or on the leg, and the same system can be used to monitor muscle activity (EMG). The patch of size $60 \times 20$ mm$^2$ includes a microprocessor, a 2.4 GHz radio link, and a miniaturized rechargeable lithium-ion battery. Data are sampled nonstop between 250 and 1000 Hz, and the battery has a capacity of 175 mAh adequate for several days.

Sensors for physiological conditions is designed for personal health and general environmental monitoring to measure temperature, pressure, humidity, and vibration/position and available as a wrist strap to make it wearable system

(Fig. 16.11a). Many different versions have been adopted in military, navy, and marine applications. Smart skin sensors (Fig. 16.11b) monitor health parameters such as heartbeat/pulse rate, body temperature, and acoustic waves and can be worn underneath soldiers' uniform. The RF-based wireless transmitters convey health parameters to health camp via a close-by vehicle. SHIMMER wearable mote has been developed by the Digital Health Group at Intel with TI MSP430 processor, CC2420 IEEE 802.16.4 radio, Triaxial accelerometer, rechargeable Li-polymer battery, and MicroSD slot supporting up to 2 GBytes of flash memory.

Sensor for optical motion capture (Fig. 16.12a) primarily employs reflective markers and multiple cameras that digitize different views of performance. Fiber-optic sensors (Fig. 16.12b) use rotation based on transmitted light. An embryonic method for transferring data from human body employs electronics textiles (e-Textiles) (Fig. 16.12c) as a communication medium. The medium consists of two electrically separate grids of conductive thread that could physically

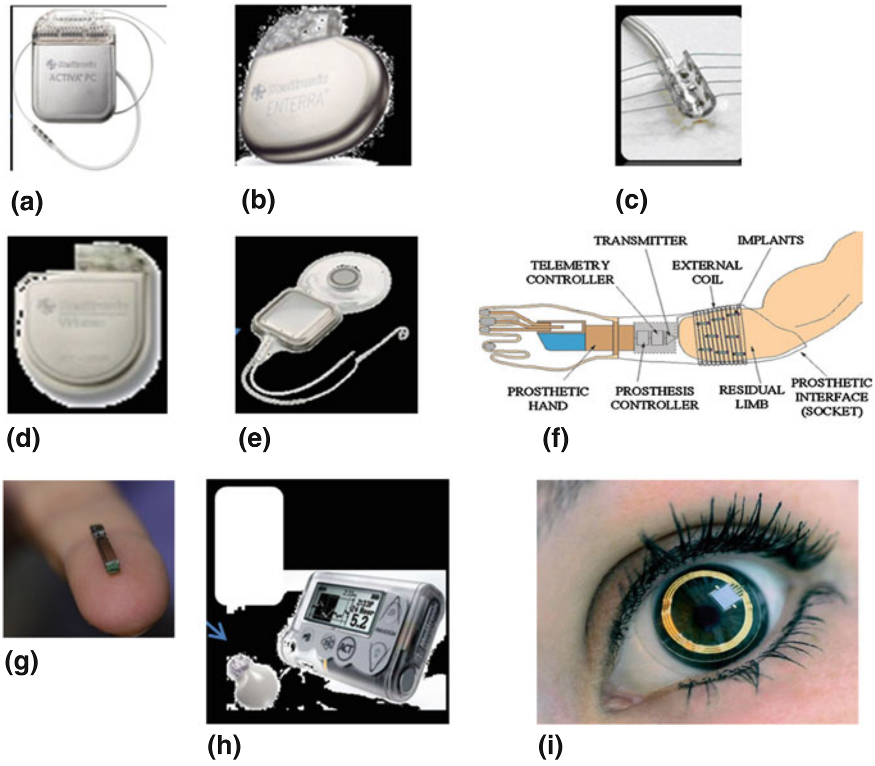


**Fig. 16.8** **a** Deep brain Neuro-stimulator **b** Gastric stimulator **c** Foot drop implants **d** Cochlear implants **e** Cardiac defibrillator/pacemaker **f** Artificial hand **g** Implantable glucose sensor **h** Insulin Pump **i** Artificial Retina

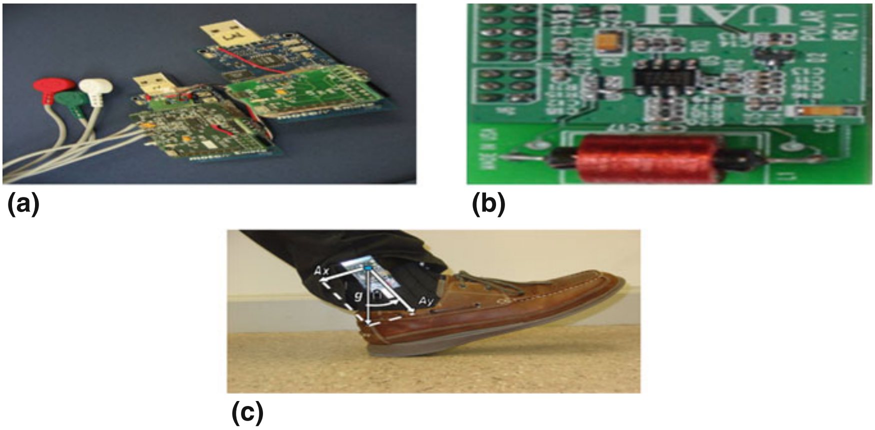

Fig. 16.9 **a** ECG **b** EMG **c** Motion sensing

connect SNs to the shared medium using metallic button-snaps and communicate via an e-Textiles transceiver chip. The use of a pair of physical low-impedance connections has the distinct advantage as it enables to connect signal differentially, permitting energy-efficient amplitude-modulation schemes that tolerate coupled interference and power SNs remotely from a local BS. Objects for posture determination shown in Fig. 16.13 can be for the whole human body, portions of the body, facial animation, and for animals or puppets.

## 16.4 Parkinson's Disease and Fatigue Level Detection

Parkinson's disease affects about 3% of the population over the age of 65 years, and NIH reports suggest that more than 0.5 million people affected in the USA and 4–6 millions in the world. There is no cure for Parkinson's disease. Even though Parkinson's disease is hereditary, early detection can improve the mortality rate. Early symptoms include mild tremors, problems with balanced walking, and no expression on face. Changes to patient's mobility can be detected with sensors and can be used to determine the onset of the disease. In a recent project [5], pressure sensors embedded in the patient's shoe soles can be used to measure the amount of pressure on the patient's feet (Fig. 16.14). The data obtained can be compared to that of a healthy person to determine the degree of unbalance during walking and freezing of gates (FoG) in Parkinson's patients can be determined with changes in pressure and data over time can be used to determine the progress of the disease. The sensor data can be recorded in real time, and the doctor can use the data for a better diagnosis. Pressure sensors embedded in the patient's shoe soles can be used to measure the freezing of gates as electronic circuit is hidden in the shoe sole (Fig. 16.15).

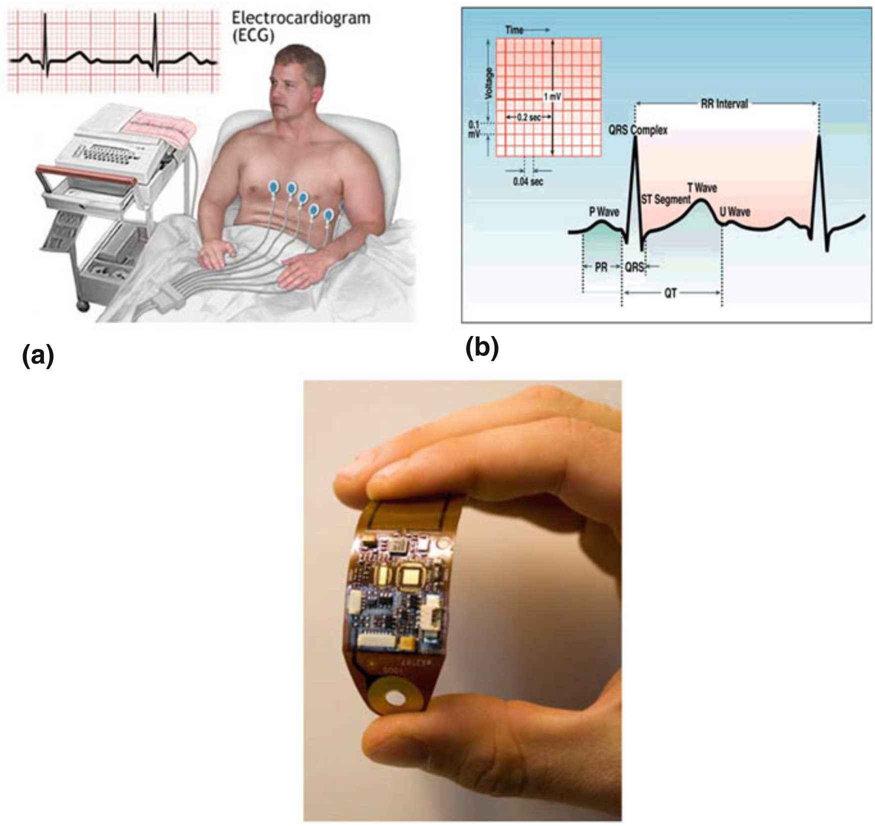


**Fig. 16.10** **a** ECG set up **b** ECG waveform **c** IMEC patch

Monitoring Athlete's during their practice and game sessions is important for the captain and owners. It is critical to monitor how tired a player is and when to make a player rest by replacing by a new one and vice versa. Therefore, general health monitoring while in action is critical. A recent work [6] employs 9 pressure sensors embedded in the shoe soles that can be used to measure the amount of pressure on the player's feet and conveyed to the coach sitting on sidelines. Data obtained from two feet are compared to determine the degree of fatigue during playing, and changes in the pressure data over time can be used to determine time to change with a resting player. The sensor data can be obtained in real time by the coach and take a player out/in. The scheme can be useful for areas where uninterrupted long hours are needed such as nurses, doctors, army and defense personnel, and truck drivers.

In a similar way, helmet is being used by football players for avoiding concussion due to the impact on head by injuries (Fig. 16.16a) and integrated assembly equipped with thermal sensors, video cameras, and chemical and biological sensors is commercially available. So, efforts are being made in monitoring potential health

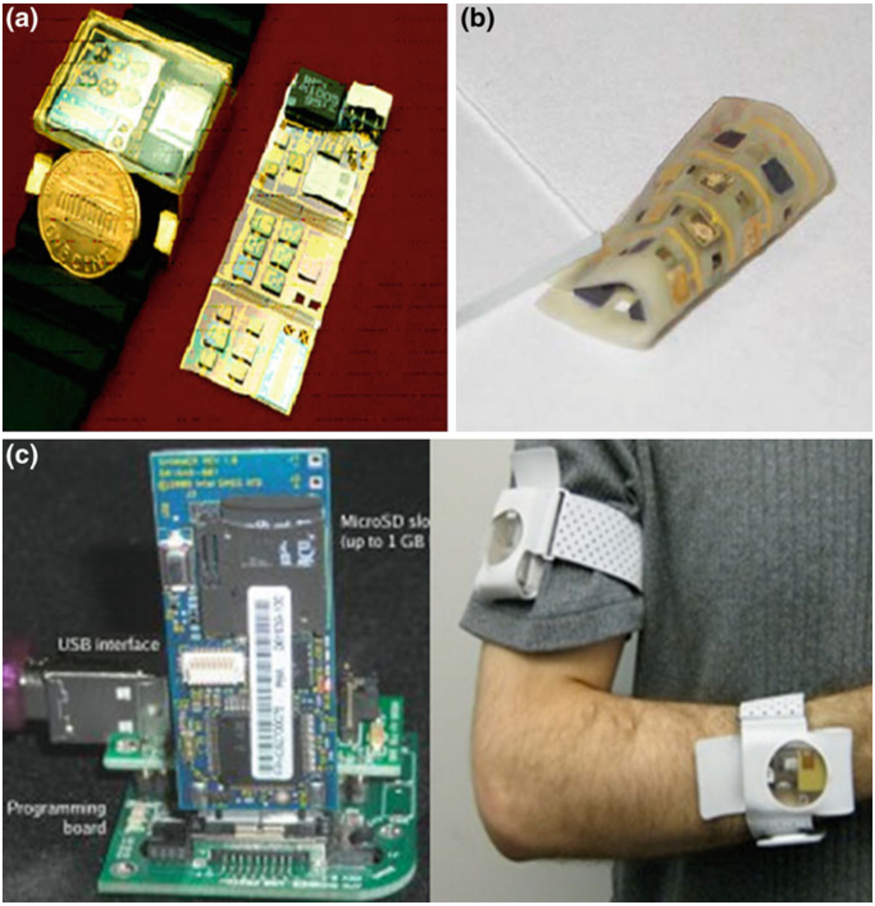


**Fig. 16.11** **a** Wrist Strap for physiological conditions [15] **b** Smart skin sensors [16] **c** SHIMMER wearable mote [17]

problems due to different factors. But, once diagnosed, same amount of medicine is prescribed for duration of more than a week, commonly for a month, and no change in medication is done for extended period of time. Therefore, there is a need to monitor patient's condition 24/7 and accordingly adjust the medication doses as needed. Such a future system is illustrated in Fig. 16.16b.

## 16.5 Communication Through Skin

To monitor physiological parameters, SNs can be mounted on or implanted inside human body and transfer data to healthcare provider or doctor for analysis in multi-hop fashion. One such deployment is shown in Fig. 16.17, and irrespective of


**Fig. 16.12** **a** Reflective Markers **b** Fiber optic sensors **c** e-Textile SNs

employed routing protocols (Table 16.4), SN in operation will cause heat rise in the surrounding vicinity as transmission, reception, and relaying of packets cause an increase in temperature. This is independent of underlying MAC protocol (Table 16.5). If heat rise is > thermoregulation, then tissues could be damaged. In order to obtain a mathematical mode for the heat rise, Pennes bio-heat equation [7] is given as follows:

$$C_P \frac{\partial T}{\partial t} = \nabla(K\nabla T) + A_0 + B_0(T - T_b) + \rho(SAR) + P_D, \qquad (16.1)$$

where T is the temperature in °C, $K$ is the thermal conductivity(J/(ms °C)), C is the specific heat(J/(kg °C)), $A_0$ is metabolic rate, $B_0$ is the blood perfusion constant(J/($m^3$ s °C)), TB is the temperature of the blood in °C, and PD is the power dissipated

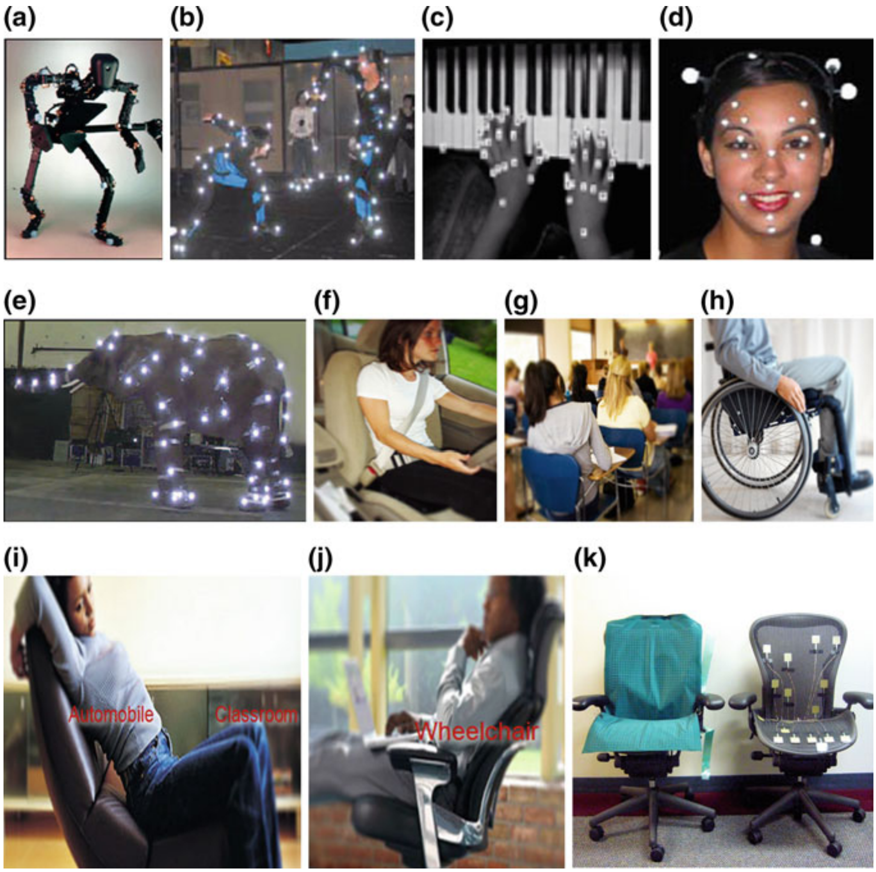


**Fig. 16.13** **a**, **b** Human whole body **c** Portions of body **d** Facial animation **e**, **f**, **g**, **h**, **i** Sensors for seated postures **j** Original chair and chair with Sensors

over a volume. Temperature of different parts of the body does increase and is summarized in Table 16.6. Most existing work assumes each SN to have a fixed awake time $(t_A)$. A sleep-awake cycle scheme has been proposed [8] which combines both thermal awareness and generating of efficient duty cycle by proposing a heat-based MAC protocol. Given a WBAN, set a fixed awake time for each of the SNs, termed as *sampling window* for each SN. Once a SN has its *sampling window period*, it goes to sleep. The duration of its sleeping period $(t_s)$ is given by the following equation:

$$t_s = PDF(\Delta T), \tag{16.2}$$

where PDF is the probability distribution function. There are many possible sleep models that indicate the *amount of time SNs sleep* such as *Poisson*, *Binomial*,

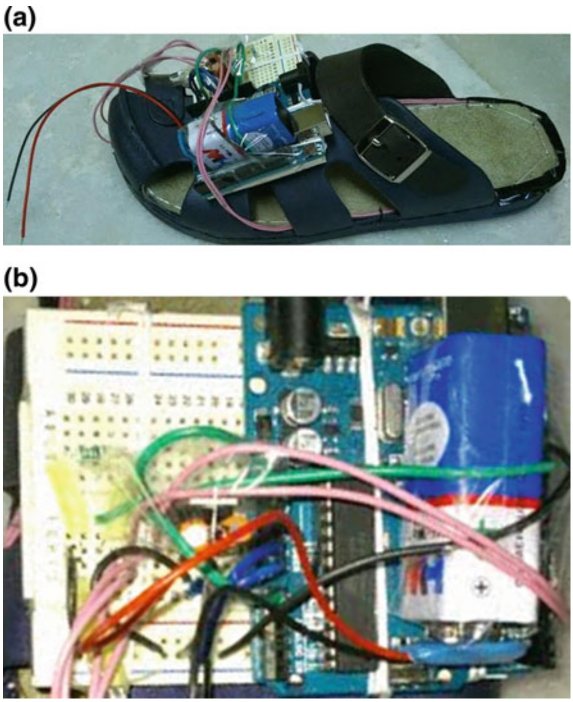


**Fig. 16.14** **a** Shoe to determine FoG **b** Electronic circuitry inside shoe sole

*lognormal*, *and Laplace*. PDFs are able put the SNs to sleep for a longer period based on the temperature rise. These PDFs have been tried to check which provides a better throughput as a function of network size (Fig. 16.18a). Figure 16.18b shows the average temperature rise of the network when the sampling window time is increased. The network size is set to 3 × 3 2-D mesh and simulated for 1000 s by varying the value of sampling rate from 1 s to 5 s. Figure 16.18c shows the temperature rise of each node along the y-axis with a sampling rate of 5 s which clearly shows that Node 5 has a peak temperature increase as this is the busiest node in terms of this network. Figure 16.18d shows variation in sleep time over SNs. It is observed that Node 5 indeed sleeps for around 30% of the time in Poisson, Binomial, and Laplace distributions and 40% of time in case of the lognormal distribution. It may be noted that the grids are portions of human tissue that are able to transmit heat through convection and radiation constantly that makes SNs to be constantly heated up, even after packet loss (Fig. 16.19).

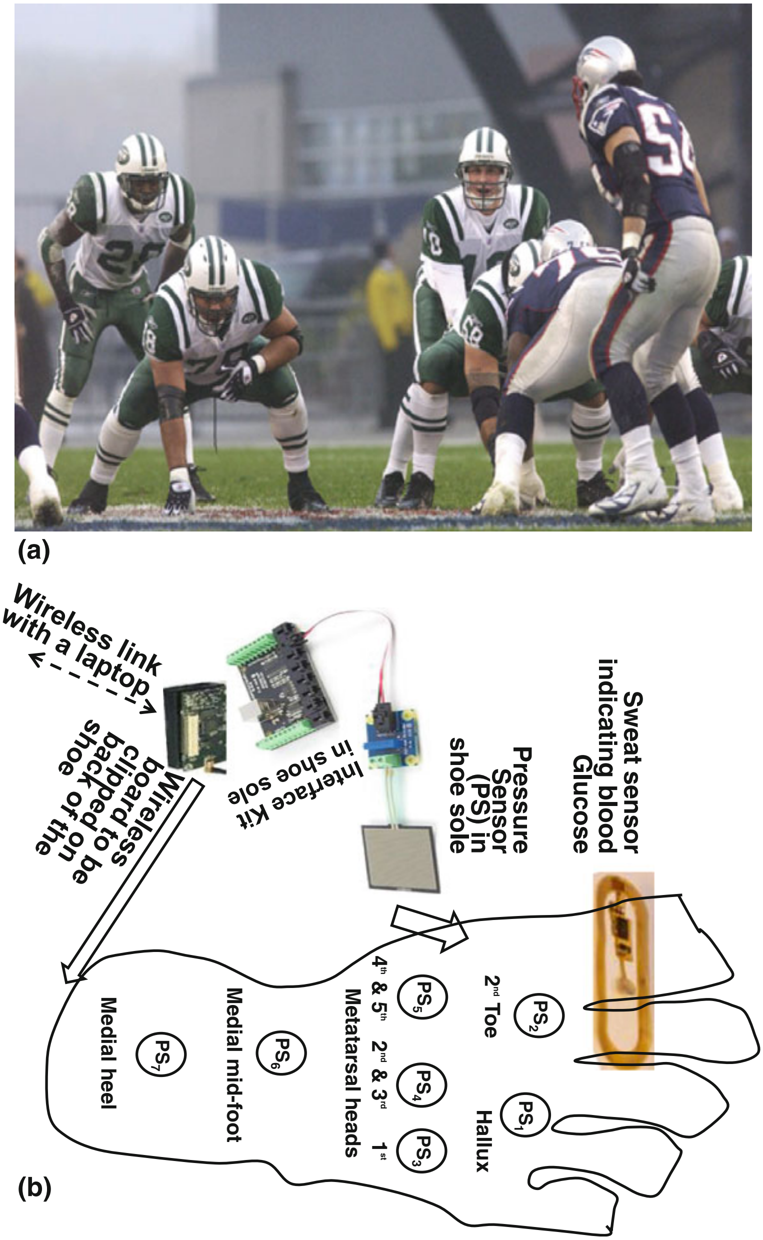


**Fig. 16.15** **a** Players at football game **b** Shoe with 7 pressure sensors [6]

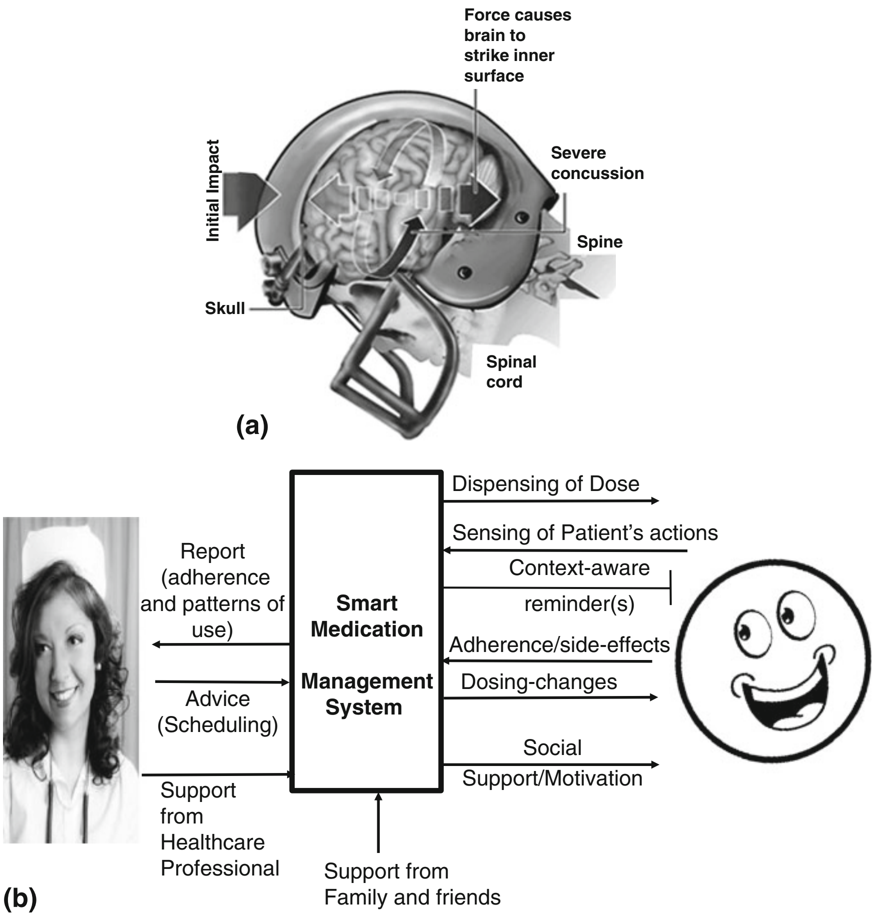


**Fig. 16.16** **a** Helmet and concussion **b** Medication Monitoring

## 16.6 Interference in WBANs

When multiple WBANs are present close by, then there will be interference as other SNs could concurrently transmit within the transmission range of a sender SN. Two types of interference are possible: intra-WBAN interference and inter-WBAN interference (Fig. 16.20). Both intra-WBAN and inter-WBAN interferences are due to cochannel interference that could lead to critical data loss, which can prove to be life-threatening to patients using these devices for health monitoring. This is also a severe threat to reliability of the network functioning and is a security threat for the patient's personal data. Attempts have been made to increase throughput in the WBAN. These include opportunistic packet scheduling, variable TDMA scheduling, and random and incomplete coloring algorithm. The energy consumption of

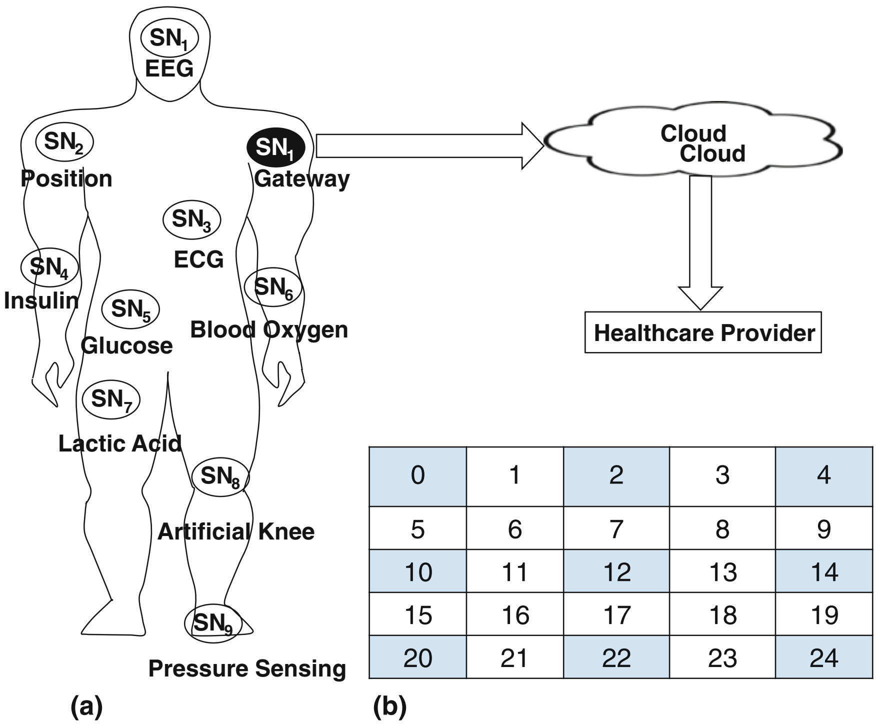


**Fig. 16.17** **a** Transferring Physiological data using SNs **b** Coordinator Model on human body with 25 SNs

**Table 16.4** Thermal aware routing in WBAN [18]

| Protocol | Routing decision | Network temperature | Nodal temperature | Packet drops |
|---|---|---|---|---|
| TARA | Per-hop | High | Moderate | Yes |
| LTR | Per-hop | Moderate | Low, High$^{w}$ | Yes |
| ALTR | Per-hop | Moderate | Low, High$^{w}$ | No |
| LTRT | End-to-end | Moderate | Moderate | No |
| HPR | Per-hop | Moderate | Low | No |
| TSHR | Per-hop | Moderate | Low | No |
| SHR | Per-hop | High | High | No |

$^{w}$Worst case

SNs is too high in opportunistic scheduling, and most schemes do not address the issues of transmission losses due to unpredictable human mobility. None of the existing models use IEEE 802.16.6 standard which is designed especially for WBAN ensuring QoS. So, two schemes [9] have been suggested to mitigate interference in WBANs. Intra-WBAN interference mitigation is achieved by Fuzzy inference reasoning and decision making for allocating transmission slots

**Table 16.5** MAC protocols and metrics [19]

| Metric | CSMA/CA | TDMA |
|---|---|---|
| Power consumption | High | Low |
| Traffic level | Low | High |
| Bandwidth utilization | Low | Maximum |
| Scalability | Good | Poor |
| Synchronization | N/A | Required |

**Table 16.6** Temperature increase in human body with implanted coil dissipating 984 μW [20]

| Tissue | Maximum temperature rise °C |
|---|---|
| Retina | 0.025 |
| Skin | 0.089 |
| Fat | 0.152 |
| Bone | 0.018 |

(Fig. 16.20b, c), while inter-WBAN interference mitigation is achieved by a decentralized cooperative scheduling approach for mobile WBANS, among the interfering coordinators to ensure non-overlapping transmission slots.

Three input variables of sensor signal-to-noise ratio  in dB, bit error rate ratio, and energy per bit to noise power spectral density ratio corresponding to all *n* SNs in the WBAN are used to have a unique output decision that maps to either of the three possibilities, namely "defer," "schedule," or "forward," data and defuzzifier is not required in this approach. The inputs are BER ⊂ {too high, acceptable, good}; SNR ⊂ {dangerous, just-okay, better}; and $E_b/N_0$ ⊂ {critical, boundary, superior}, while the output decision is ⊂ {defer, schedule, forward}. The Fuzzy interference table is given in Table 16.7. Decision considers two parameters BER and $E_b/N_0$.

BER and SNR are given in Fig. 13.21.

Inter-WBANs interference is present when two or more WBANs are within the interference range of one another Fig. (16.21). Each SN sends data to its coordinator in their own scheduled slot time. If two WBANs using the same frequency channel are overlapped, the received SINR of some SNs at the coordinator will be below threshold which is unacceptable. Thus, a cooperative scheduling among WBANs is required to mitigate interference (Fig. 16.22a). Shox network simulator used [9] to set up multiple WBAN scenarios with 25 SNs is strategically placed in 10 m × 10 m area. There are local coordinators (LCs), and other nodes are used for sensing, variable data rates up to 250 kbps. The properties of physical and MAC layers are set according to IEEE 802.15.4 standards. The SNs movement is decided by setting Random Waypoint Model (RWPM). A variable disc model is used in which the receiver receives packet with a signal strength  of $s(rx) = s(tx)/d\hat{A}^2$, where d is the Euclidean distance between sender and receiver SNs pair. A number of messages are exchanged in the decision process as time elapses, which is given in Fig. 16.22b, c.

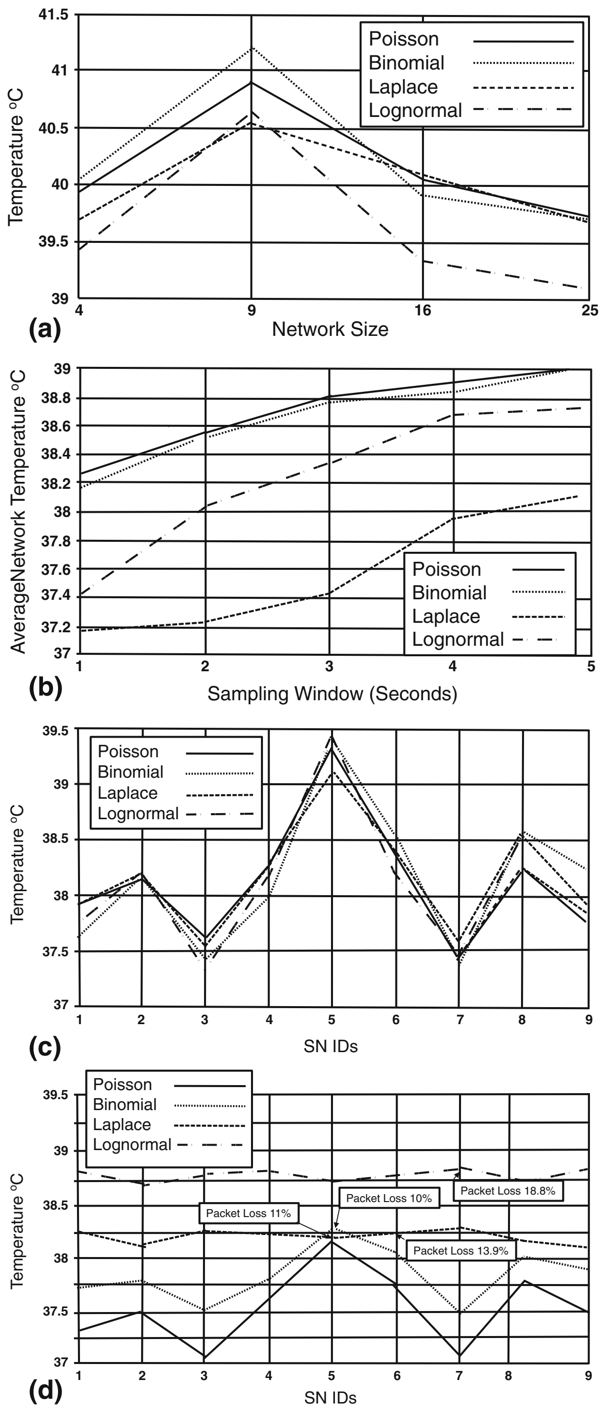


**Fig. 16.18** **a** Variation of Temperature versus Network Size **b** Temperature versus sampling window **c** Temperature versus ID of SNs **d** Sleep Duration versus ID of SNs

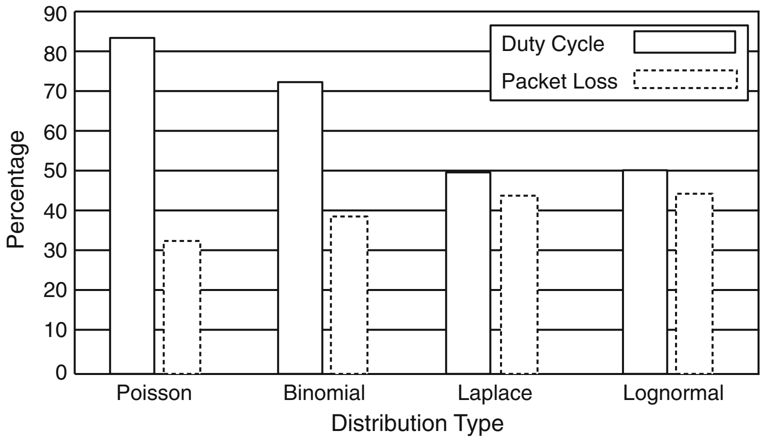


**Fig. 16.19** Duty cycle and packet loss

## 16.7 Data Reduction Schemes

Table 16.8 shows encoding of two physiological signals: pulmonary artery pressure (PAP) and ECG. These could be sent through SMS messages. As there is a limit of 160 textual characters in SMS, 3600 samples for 10 secs would need 24 messages. One possibility is to utilize short-duration PAP and ECG signals. Another alternative is to skip some of the frames without affecting the final outcome, and a sample reduction by a factor of 5 would lead to only 5 SMS messages. To enable skipping of frames, architecture has been proposed [10] as shown in Fig. 16.23.

A WBAN with a coprocessor is used as an additional microcontroller for data logging, processing and temporary storage of data samples. Smartphone is used as the Coordinating Sink Station (CSS). Wireless extension/add-on for SN communicates with the CSS over GSM. SNs sense and process the physiological data, encode, pack as a text message or as a voice-coded data message, and pass on to GSM extension. The extension transmits the data to the smartphone CSS. CSS can make decisions regarding a need-based use of voice/data network instead of WBAN links. Another important functionality is the use of speech signal encoding of the physiological sensor data using PSK and transmission as a voice call. The coprocessor sends encoding request to the signal processor which acknowledges the request and generates a digitally modulated output of the compressed sensor data using BPSK. This encoding uses human speech frequencies (100 Hz–3.3 kHz) in digital modulation. The generated output is a human voice signal, and Arduino microcontroller board with a GSM shield extension provides necessary interface. Four different subsets are derived from original PAP and ECG signals, with the first subset retains alternate samples, the second contains every third sample, the third set has every fourth sample, and the fourth has every fifth sample (Fig. 16.24). The reduced samples by skipping frames is compressed, encoded, and transmitted as

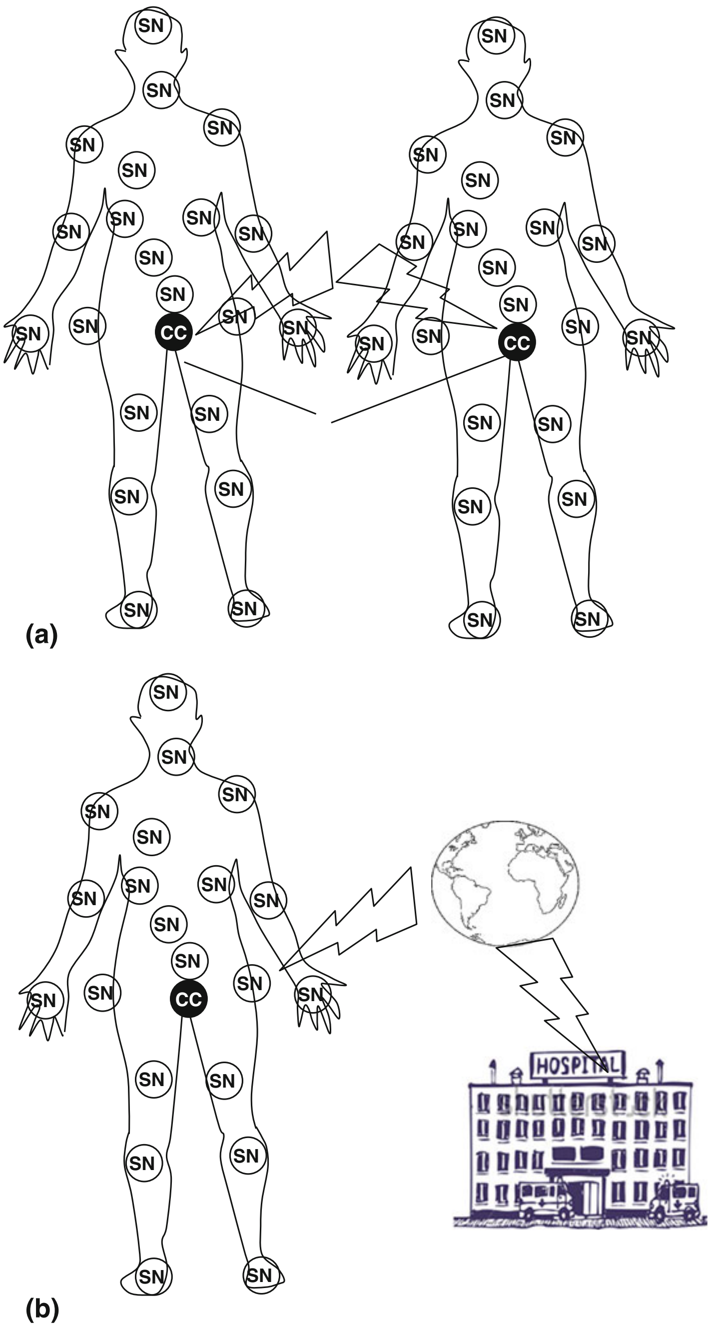


**Fig. 16.20** **a** Interference in WBANs **b** Intra-WBAN Interference **c** A General Fuzzy Logic System

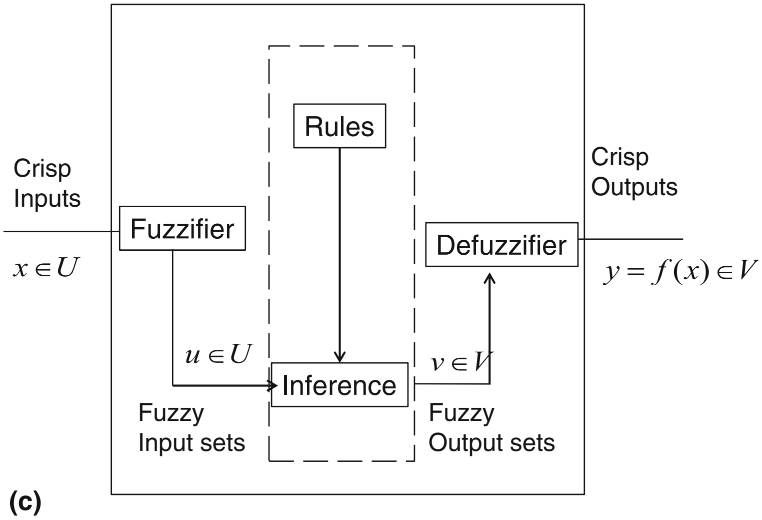


**Fig. 16.20** (continued)

**Table 16.7** Fuzzy inference table

| BER | SNR | | | $E_b/N_0$ |
|---|---|---|---|---|
| | Dangerous | Just-okay | Better | |
| Too high | Defer | Defer | Defer | Critical |
| Too high | Defer | Defer | Defer | Boundary |
| Too high | Defer | Defer | Schedule | Superior |
| Acceptable | Defer | Schedule | Schedule | Critical |
| Acceptable | Defer | Schedule | Schedule | Boundary |
| Acceptable | Forward | Schedule | Forward | Superior |
| Good | Forward | Forward | Forward | Critical |
| Good | Forward | Forward | Forward | Boundary |
| Good | Forward | Forward | Forward | Superior |

text messages over GSM network. At the receiving end, the encoded and compressed BAN data is processed to rebuild the original samples. Missing samples are recreated using five numerical interpolation techniques. The nearest-neighbor interpolation algorithm has higher errors, while linear spline interpolation performed better on data sets (Fig. 16.24).

Another approach for minimizing physiological data is to do aggregation in time domain [11] using regression polynomial discussed in Chap. 10. A fourth-order polynomial can be written as:

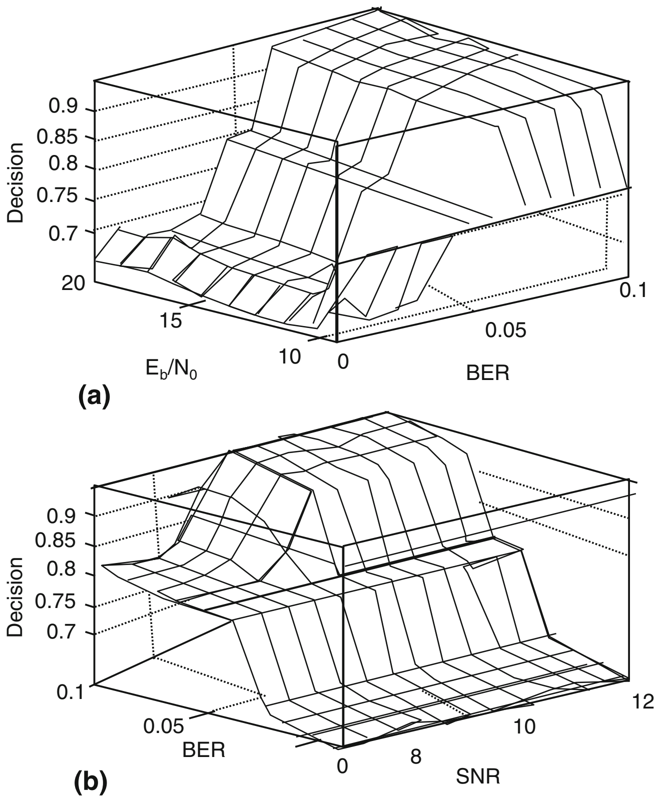


**Fig. 16.21** Intra-cluster Decision based on various Input parameters **a** BER and $E_b/N_0$ **b** BER and SNR

$$f(t) = \beta_0 + \beta_1 t + \beta_2 t^2 + \beta_3 t^3 + \beta_4 t^4. \tag{16.3}$$

and eighth-order polynomial as:

$$f(t) = \beta_0 + \beta_1 t + \beta_2 t^2 + \beta_3 t^3 + \beta_4 t^4 + \beta_5 t^5 + \beta_6 t^6 + \beta_7 t^7 + \beta_8 t^8, \tag{16.4}$$

where $\beta'$ s are constant coefficients and f(t) is the value at time t.

A fourth-order polynomial can be easily created by the following matrix:

$$\begin{bmatrix} y_1 \\ y_2 \\ \vdots \\ y_n \end{bmatrix} = \begin{bmatrix} 1 & t_1 & t_1^2 & t_1^3 & t_1^4 \\ 1 & t_2 & t_2^2 & t_2^3 & t_2^4 \\ \vdots & \vdots & \vdots & \vdots & \vdots \\ 1 & t_n & t_n^2 & t_n^3 & t_n^4 \end{bmatrix} \begin{bmatrix} \beta_0 \\ \beta_1 \\ \beta_2 \\ \beta_3 \\ \beta_4 \end{bmatrix} + \begin{bmatrix} \varepsilon_1 \\ \varepsilon_2 \\ \vdots \\ \varepsilon_n \end{bmatrix} \Leftrightarrow \vec{y} = T\vec{\beta} + \vec{\varepsilon}. \tag{16.5}$$

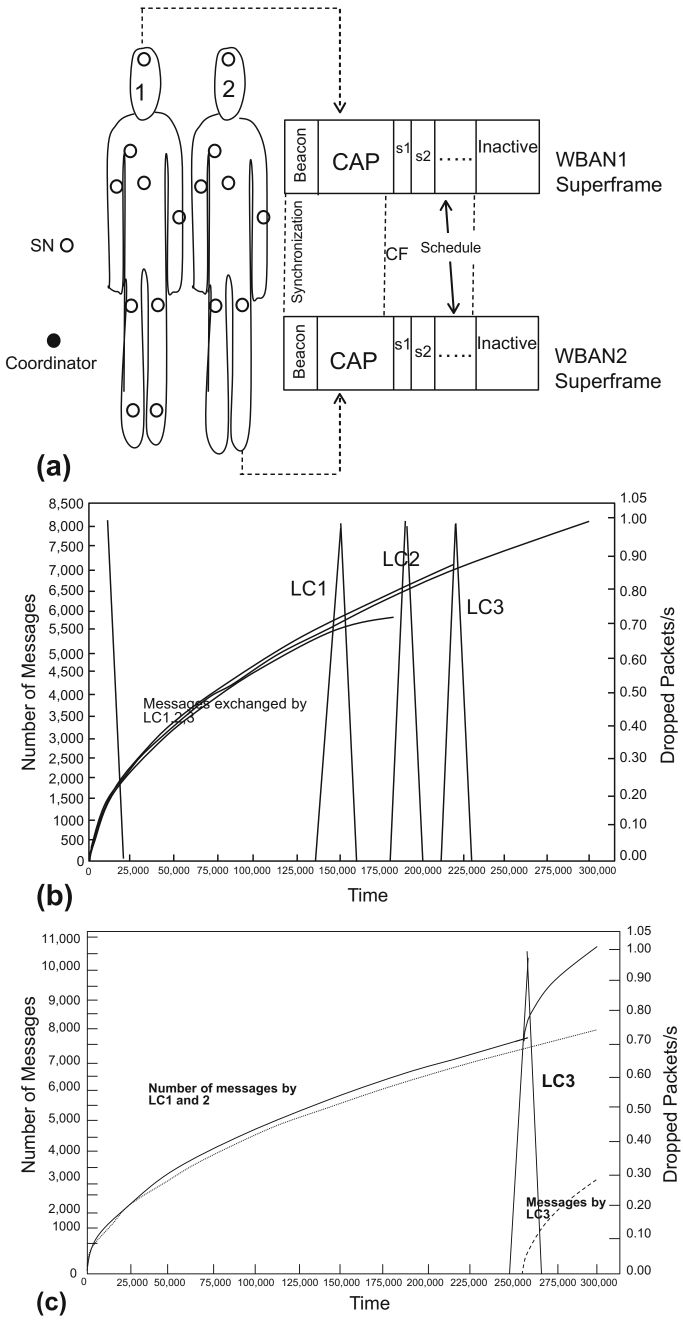


**Fig. 16.22** **a** Inter-WBAN Interference **b** Interference effects with no MAC scheduling **c** Interference effects with TDMA -MAC scheduling

**Table 16.8** Encoding for the two physiological signals

| Physiological parameter | Range (mV) | Span (mV) | Step size (8bit encoding) (MuV) | Max encoding error (MuV) |
|---|---|---|---|---|
| PAP | 20–45 | 25 | 97.6 | 48.8 |
| ECG-II | −0.75–0.0 | 1.75 | 6.83 | 3.41 |

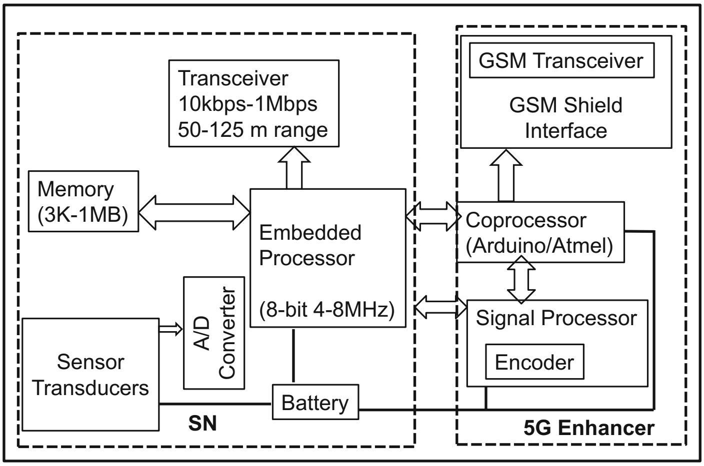


**Fig. 16.23** Proposed architecture for skipping frames

Then,

$$\widehat{\vec{\beta}} = \left(T^{\mathbb{T}}T\right)^{-1}T^{\mathbb{T}}\vec{y}, \tag{16.6}$$

where $\widehat{\vec{\beta}}$ is an estimate of the original coefficients. This has been used for 4 types of biological data, blood pressure, EEG scalp readings, motor movement signals, and motor movement signals in patients with neurodegenerative disorders. The accuracy is measured for both fourth-order and eighth-order polynomials (Fig. 16.25). Eighty blood pressure samples are taken at 0.01 s intervals and 80 samples in μV are taken for motor movement at 0.0039062 s intervals, while the sample size of Degenerative Gait EEG Readings is 300, and measures signals in mV are obtained from the left leg at 0.0033333 s intervals.

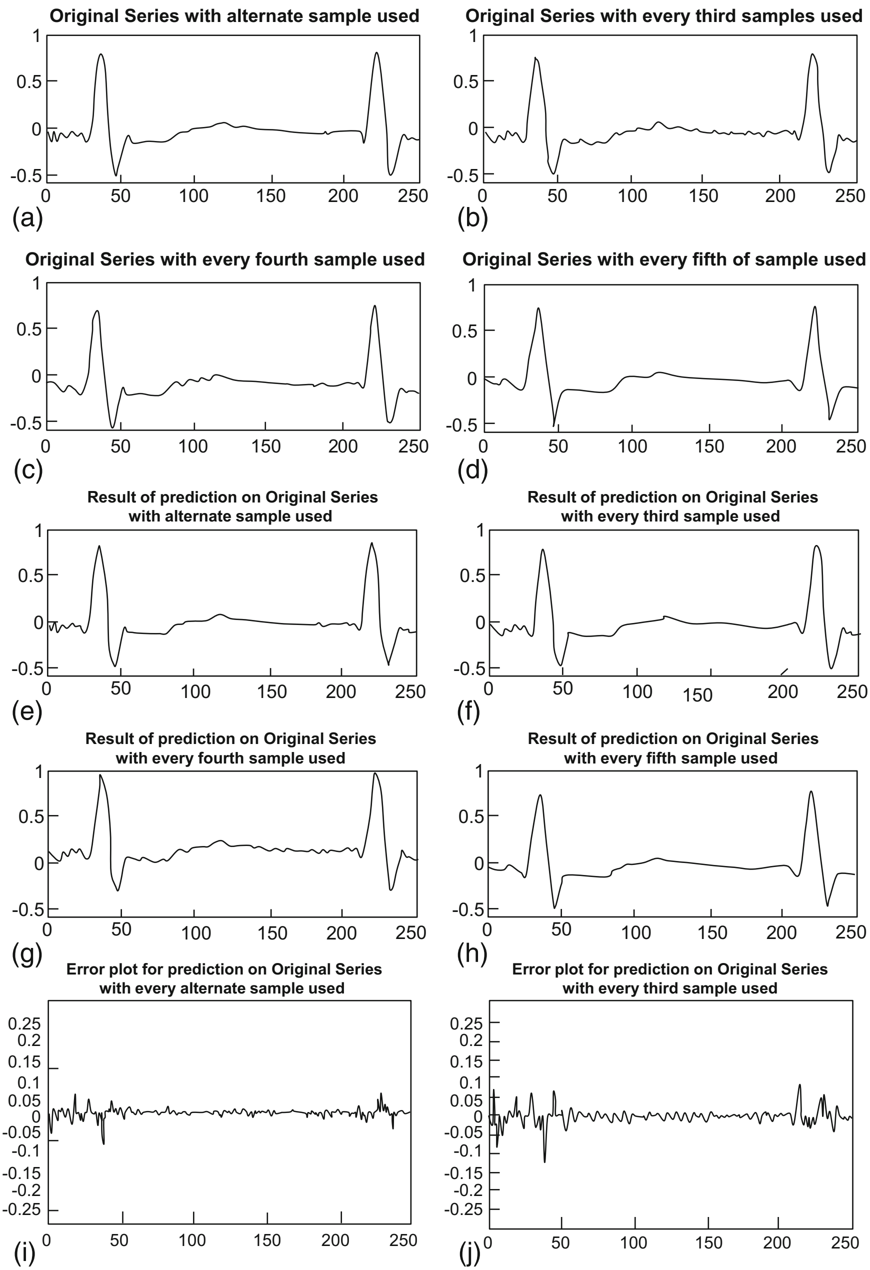


**Fig. 16.24** **a**, **b**, **c**, **d** Original ECG samples **e**, **f**, **g**, **h** Rebuilt ECG Signals **i**, **j**, **k**, **l** Error for Recreated ECG data **m**, **n**, **o**, **p** Original PAP signals **q**, **r**, **s**, **t** Error for Recreated PAP data

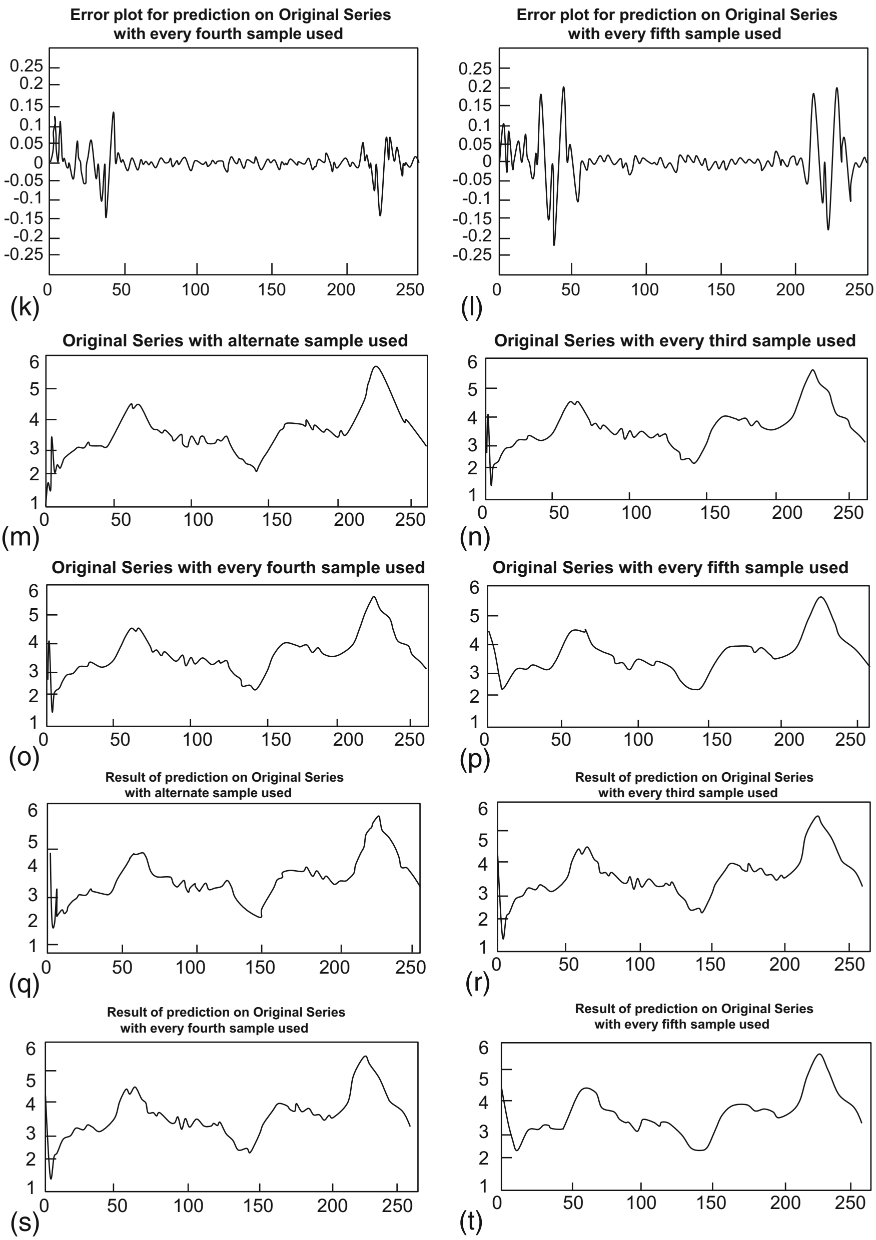


**Fig. 16.24** (continued)

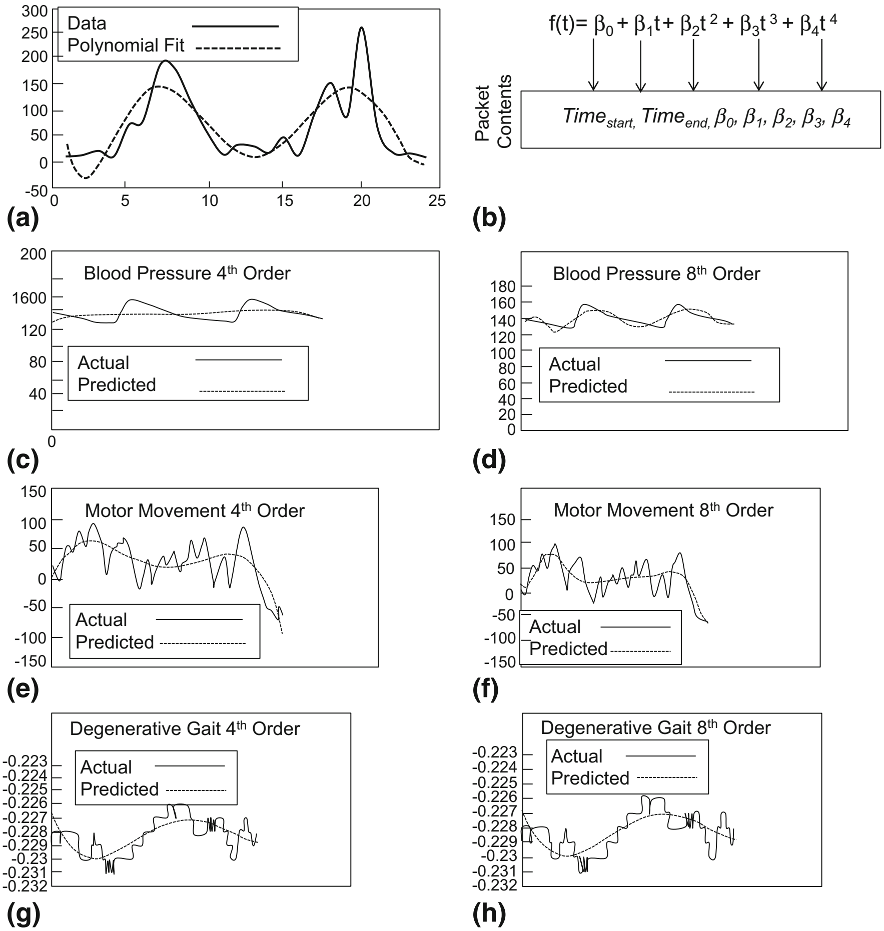


**Fig. 16.25** **a** A generic Aggregation with Polynomial Regression **b** 4th order example **c** Blood Pressure **d** EEG Scalp **e**, **f** Motor movement **g**, **h** Neurodegenerative Motor Movement

## 16.8 Physiological Parameters for Identification Secured Communication

The traditional biometric approaches make use of distinct physiological characteristics of a person and use the same to determine their identity. This entire process is termed as biometric authentication [12]. The most conventional parameters involve physiological characteristics ranging from noninvasive features such as facial and hand geometry to invasive techniques such as impression from a finger, the distinction of an iris, or the structure of the DNA. Some behavioral patterns also find application in identity association such as voice modulation and acoustics, the mechanics of locomotion, keystroke dynamics, and one's penmanship. In general, biometric parameters are qualified by: *invariance*, *measurability*, *singularity*, *acceptance*, *reducibility*, *reliability*, *and privacy.* Given such considerations, the numbers of such parameters which find applicability are few. A point to be taken into consideration is that biometric systems are not perfect nor are they designed to be so; additionally, there are two error metrics commonly associated with biometrics: FAR (false accept rate) and FRR (False Reject Rate) [13]. FAR refers to the probability of generating a false positive, which is wrongly identifying and accepting an impostor for a genuine user. FRR refers to the probability of mistakenly rejecting a valid user. These two parameters jointly serve as tools which can gauge the overall performance of a biometric feature in action. A third parameter at which the false rejection rate and the false acceptance rate are equal also acts as a metric for determining the accuracy of a biometric system known as equal error rate.

Over the years, several researchers have concluded that the study of a person's gait is adequate to determine their gender and identity. Most of the research in the analysis of gait has been limited to the usage of photography and video capturing devices, limiting the study to spatiotemporal components. Gait recognition techniques can be broadly classified into three categories: (a) machine vision (MV) based, (b) floor sensor (FS) based, and (c) wearable sensor (WS) based. MV-based gait analysis techniques usually incorporate studying the silhouette of a person as capture on reel. Usually, the parameters of interest are stride, cadence, height, proportions of bodily features and, the overall silhouette of the person. The cameras used for studies could be video or infrared or a combination of both, depending upon use. The main idea behind such monitoring model is to breakdown movement into a collection of joints and their functioning, thus computing the angular motion of each component during motion. These involve the placement of floor-mounted load transducers, commonly referred to as force sensors. Such a platform is responsible for measuring the ground reaction forces along with the direction, magnitude, and location of the applied pressure. While this technique

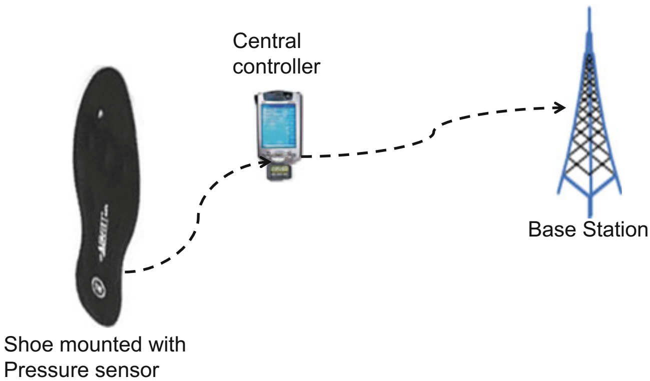


**Fig. 16.26** Architecture for Gait Monitoring

does satisfy the properties that make a good biometric, the infrastructure costs involved render this technique economically unfeasible, thus preventing it from finding application in real life. WSN-based techniques usually involve the usage of inertial sensors such as accelerometers and gyroscopes to study the human form while in motion. The purpose of this technique is to apply the motion sequence generated by the lights to identify the wearer, thus providing a large scope for biometric applications.

Person's stride interval is used as a biometric and can be achieved by placing pressure sensors in the sole of the person's shoe (Fig. 16.26). By virtue of its placement, every footstep taken is recorded; as such, the time lapse between steps can be monitored and processed. A standard pressure sensitive floor is not the preferred tool of choice given its high susceptibility to external noise and subjectivity to exterior motion. As such, on-body sensors allow the sensed data to be localized to only the user concerned, allowing for improved identification and authorization. A critical feature of this model is to insure that the sensor cannot be felt by the user, which may lead to consciousness and discomfort. Given its inconspicuous positioning, this system can be easily deployed on humans, ready to adapt to everyday living.

While the limitations of gait are known, we propose using gait as a passive biometric, paired with another feature rather than being used in isolation. However, before we investigate the merits of the latter, in this research we will be discussing the benefits of using gait alone.

The data set is analyzed by employing statistical measures for the purposes of establishing consistency and uniqueness and to derive its characteristics precisely. Based on the available data, distribution of the stride interval values for (a) a user and (b) across multiple users has to be determined. In the former case, the stride interval generated by each of 10 users follows a normal distribution (Fig. 16.27). This implies that a particular user tends to follow a rhythmic motion, and each step is almost equally spaced apart, following a normal distribution. Theoretically, the probability density function is given by:

$$f(x) = \frac{1}{\sigma\sqrt{2\pi}} \exp^{-\frac{(x-\mu)^2}{2\sigma^2}} \tag{16.7}$$

The parameter μ $\psi$ is the expectation value against the sensed data; σ $\psi$ refers to the standard deviation about the mean. It can be concluded that humans in motion tend to adopt a two-dimensional Gaussian distribution. As shown in Fig. 16.27, a Gaussian density function is made available at each data point, and over the range of the data, the sum of density functions is computed. Considering the randomness of the sensed data, data from different users exhibits a bell-curve distribution, with the trend for each user being localized around a mean. With every user in consideration, the distribution plot is plotted and a normal distribution can be obtained. Although the distribution function for each group is not uniform, the three means for each user are largely centric about a similar mean. The *stride interval* exhibits long-range power-law correlations which indicate a fractal process model

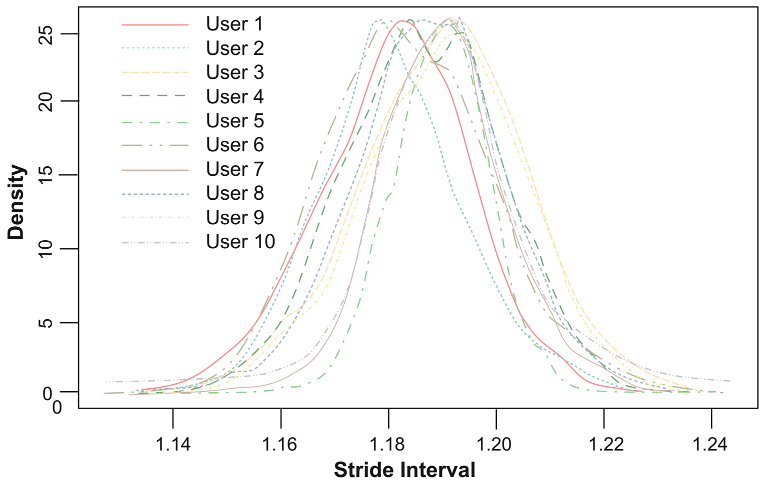


**Fig. 16.27** Demonstration of Density Estimation

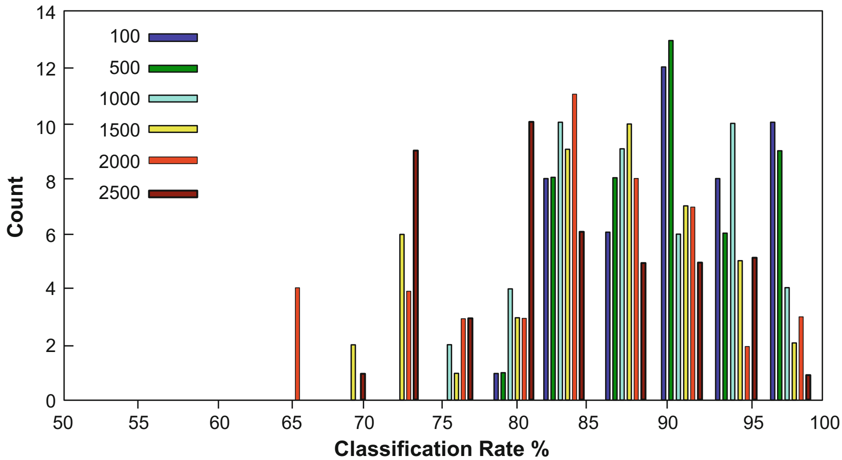


**Fig. 16.28** Variance of positive classfication rate for various sample sizes

assumptions that we make when we apply gait as a biometric is that each recorded value can be modelled as a normal random variable that each occurrence of a statistic is statistically independent and, finally, that each result obtained traces back to a population having the same variance. To perform the summary analysis, a one-way ANOVA (analysis of variance) was carried out with alpha $>\psi$ 0.05, exhibiting statistical significance. The results from the ANOVA runs are very promising and confirm the fractal nature of human strides.

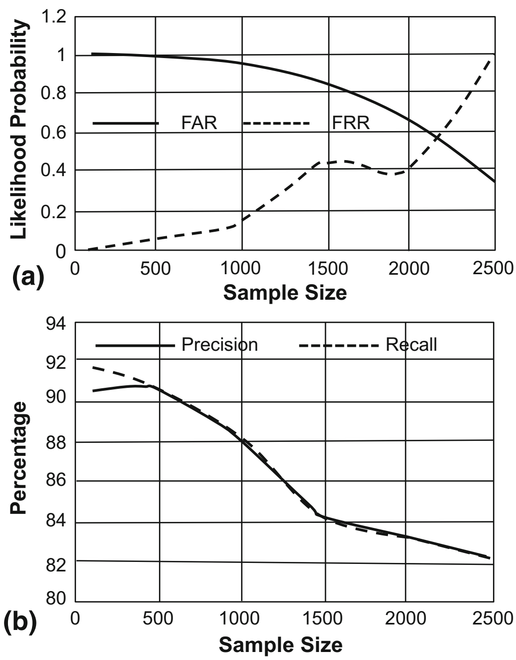


**Fig. 16.29** **a** Results of GMM classification **b** Precision vs Recall from GMM classification

Given that authentication is the main goal behind applying Gaussian Mixture Models (GMMs) [14], the gait model should be such that it can produce a low FRR and FAR. Additionally, confusion matrix and classification performance rate are generated which are used to compute the acceptance/rejection parameters. The results for FRRs and FARs for 220 samples (obtained from Monte Carlo methods) are shown in Fig. 16.28. A key feature to be noted is that the algorithm should fare well for computing FRR and FAR over time. The results depicted show the variance of FRR and FAR over a varied sample space (from 100 samples to 2500 samples) (Fig. 16.29). These values span across a range from 0.1 to 8.0% using the aforementioned features. Our conclusion is that smaller sample spaces exhibit better modelling prediction(s). The classification algorithm averaged 87% positive classification rate, which is reasonably high (Fig. 15.29). The trend that we observe is that FRR and FAR showed a consistent variance, thus illustrating the advantage of the adaptive modeling.

## 16.9 Conclusions

Numerous biomedical applications of transducers and SNs are feasible, and the demand and need for new areas are continuously growing. This is relatively new application area even though this has a long-lasting impact on human health. The key is to develop transducers that could function with 100% reliability and would not provide any false alarms. There is also a need for 24 × 7 unattended monitoring that poses a lot more constraints and needs to be addressed carefully. The number of SNs on human body could be limited to around 25 and could be placed not totally randomly, but not in a 2-D mesh structure either. This calls for further investigation of WPASNs and is an open area of research.

## 16.10 Questions

Q.16.1. How can you ascertain reliability in the monitoring of patient vital signals from sensors?

Q.16.2. What is the impact of stability on the results of biomedical monitoring?

Q.16.3. What impact do you expect on the WBAN performance if a patient is also moving around?

Q.16.4. What specific measures are needed to ensure security of patients' physiological data?

Q.16.5. What are the parameters that you utilize in WBAN for a biomedical application?

Q.16.6. In a WBAN, transducers are connected using wireless links to the local coordinator. Can they be hardwired to the coordinator?

Q.16.7. What are the limitations and advantages of approach suggested in Q. 16.5?

Q.16.8. What will be the impact on accuracy, reliability, delay, and interference if the number of SNs is doubled in a WBAN?

Q.16.9. In order to minimize interference, distance covered by individual SN in a WBAN ought to be reduced. On the other hand, new Bluetooth scheme is increasing the communication distance. What may be an appropriate approach for future biomedical applications?

Q.16.10. What will be the impact on performance and reliability if some transducers are embedded inside body skin while others are outside on the body?

Q.16.11. What other physiological parameters that could be used for identification of a person and associated security issues?

## References

1. Diego Martinez, Francisco Blanes, Jose Simo, and Alfons Crespo, "Wireless Sensor and Actuator Networks: Characterization and Case Study for Confined Spaces Healthcare Applications," Proceedings of the IEEE International Multiconference, Computer Science and Information Technology, 2008, pp. 687–693.
2. S. Arnon, D. Bhastekar, D. Kedar, and A. Tauber, "A comparative study of wireless communication network configurations for medical applications," IEEE Wireless Communications, vol. 10, no. 1, pp. 56–61, Feb. 2003.

3. Esteban Pino, Lucila Ohno–Machado, Eduardo Wiechmann, and Dorothy Curtis, “Real–Time ECG Algorithms for Ambulatory Patient Monitoring,” Proceedings of AMIA Annual Symposium, pp. 604–608, 2005.
4. http://www2.imec.be/be_en/press/imec-news/ecgpatch.html.
5. Anagha Jamthe, Suryadip Chakraborty, Saibal K Ghosh, and Dharma P. Agrawal, “Mobility monitoring of Parkinson’s Disease patients using Received Signal Strength Indicator (RSSI) in Wireless Sensor Networks,” IEEE-CPS The 13th International Conference on Computational Science and Its Applications (ICCSA), June 24–27, 2013, Ho Chi Minh City, Vietnam.
6. Dharma P. Agrawal, Abhinav Prakash, Suryadip Chakraborty, Anagha Jamthe, and Saibal Kumar Ghosh, “Real-time Personnel Fatigue level Monitoring,” Invention Disclosure, provisional patent confirmation no. 14/846,851 dated Sept. 7, 2015.
7. https://en.wikipedia.org/wiki/Bioheat_transfer.
8. Ashwin Ganesh Krishnamurthy, Junghyun Jun and Dharma Agrawal, “Temperature gradient search for temperature-aware routing in Bio-medical Sensor networks,” 9th International Conference on Body Area Networks, September 29–October 1, 2014 London, Great Britain.
9. A. Jamthe, A. Mishra, and D. P. Agrawal, “Scheduling schemes for Interference Suppression in Healthcare Sensor Networks,” *in Proceedings of IEEE International Conference on Communication*, June 2014.
10. Amitabh Mishra and Dharma P. Agrawal, “Continuous Health Condition Monitoring by 24×7 Sensing and Transmission of Physiological data over 5-G Cellular Channels,” Invited Paper, International Conference on Computing, Networking and Communications, (ICNC 2015) Anaheim, California, USA, Feb. 16–19, 2015, pp. 584–590.
11. Andrew Knox, Suryadip Chakraborty, and Dharma P. Agrawal, “Evaluating Polynomial Regression Based Data Aggregation in Body Area Networks,” IEEE ANTS 2014, New Delhi, Dec. 14–17, 2014.
12. R. Bolle, J. Connell, S. Pankanti, N. Ratha, A. Senior, Guide to biometrics book, WorldCat.org, 2004.
13. D. Gafurov, “Behavioral Biometrics for Universal Access and Authentication,” *Annual Norwegian Computer Science Conference*, pp. 19–21, 2007.
14. Pallavi Meharia and Dharma P. Agrawal, “The Human Key: Identification and Authentication in Wearable Devices using Gait,” report CDMC, University of Cincinnati, 2016.
15. A. Mason, N. Yazdi, A. Chavan, K. Najafi, and K. Wise, “A Generic Multielement Microsystem for Portable Wireless Applications,” *Proceedings of the IEEE,* vol. 86, no. 8, pp. 1733–1746, 1998.
16. W. Khalid, I. Hossain, S. M. Mahmud and Y. Xu, “Intelligent Vehicle Based Architecture for Real-Time Monitoring of Soldiers’ Health using MEMS Flexible Smart Skin Sensors,” Proc. 5th Annual Intelligent Vehicle Systems Symposium of National Defense Industries Association (NDIA), National Automotive Center and Vectronics Technology, pp. 59–64, June 13 –16, 2005, Traverse City, Michigan.
17. https://en.wikipedia.org/wiki/Shimmer_Sensing.
18. M Tabandeh, M Jahed, F Ahourai, and Saber Moradi, “A thermal-aware shortest hop routing algorithm for in vivo biomedical sensor networks,” In Information Technology: New Generations, 2009. ITNG’09. Sixth International Conference on, pages 1612–1613. IEEE, 2009.
19. Sana Ullah, Henry Higgins, Bart Braem, Benoit Latre, Chris Blondia, Ingrid Moerman, Shahnaz Saleem, Ziaur Rahman, and Kyung Sup Kwak, “A comprehensive survey of wireless body area networks,” Journal of medical systems, 36(3):1065–1094, 2012.

20. Gianluca Lazzi, “Thermal effects of bioimplants,” Engineering in Medicine and Biology Magazine, IEEE, vol. 24, no. 5, pp. 75–81, 2005.
21. R. Weist, E. Eils, and D. Rosenbaum, “The Influence of Muscle Fatigue on Electromyogram and Plantar Pressure Patterns as an Explanation for the Incidence of Metatarsal Stress Fractures,” American Journal of Sports Medicine, December 2004, vol. 32, no. 8, pp. 1893–1898, available online after November 23, 2004.